Mode Converter and Multiplexer with a Subwavelength Phase Shifter for Extended Broadband Operation

David González-Andrade, Raquel Fernández de Cabo, Jaime Vilas, Irene Olivares, Antonio Dias, José Manuel Luque-González, J. Gonzalo Wangüemert-Pérez, Alejandro Ortega-Moñux, Íñigo Molina-Fernández, Robert Halir, Pavel Cheben, and Aitor V. Velasco

***Abstract*—On-chip mode converters and multiplexers are fundamental components to scale the capacity of silicon optical interconnects by using different spatial modes of waveguides. Recently, we proposed a low loss and compact mode converter and multiplexer consisting of a subwavelength-engineered multimode interference coupler, tapered waveguides as phase shifter and a symmetric Y-junction. However, the narrow spectral response of the tapered phase shifter limited the device crosstalk performance. In this work, we demonstrate that the use of a subwavelength grating phase shifter with low phase-shift errors substantially reduces the crosstalk and expands the operational bandwidth. A complete multiplexer-demultiplexer link consisting of two devices in back-to-back configuration was fabricated in a 220-nm silicon-on-insulator platform. Experimental measurements of the complete link show insertion loss below 2 dB and crosstalk less than -17 dB over a bandwidth of 245 nm (1427 – 1672 nm).**

***Index Terms*—Phase shifter, mode-division multiplexing, silicon-on-insulator platform, subwavelength gratings**

I. Introduction

GLOBAL internet traffic inside cloud data centers is expected to steadily increase in the forthcoming years owing to millions of new users and devices connecting to the network, and the advent of new artificial intelligence tools for massive data processing [1]. Silicon-based optical interconnects have demonstrated a great potential to address this challenge, increasing the aggregated transmission capacity through advanced multiplexing technologies such as time, wavelength, and polarization-division multiplexing [2,3]. Mode-division multiplexing (MDM) provides a new dimension to cope with the enormous demand for broader bandwidth and faster data rates that is envisioned in the future and can complement the aforementioned multiplexing technologies by using several spatial modes as independent data communication channels [4].

Different types of mode converters and multiplexers/ demultiplexers (mux/demux) have been proposed for the silicon-on-insulator (SOI) platform, including asymmetric directional couplers (ADCs) [5-9], asymmetric Y-junctions [10,11], inverse design devices [12-14], mode evolution structures [15-17] and multimode interference (MMI) couplers [18-20]. While the advantage of ADCs is the ease of design and scalability, they suffer from narrow bandwidth and tight fabrication tolerances, particularly to over- and under-etching [5]. Bandwidth and tolerance limitations of ADCs can be alleviated by using tapered waveguides [6-9]. On the other hand, asymmetric Y-junctions have a broad operating bandwidth, but are hampered by long lengths and the finite size of the junction tip, which degrades the performance of the fabricated devices [10,11]. Inverse design devices [12-14] typically have small form factors and yield low conversion loss. Finally, mode-evolution structures based on adiabatic tapers [15-17] yield a high performance over broad bandwidths at the expense of large footprints. Alternatively, several MMI based MDM designs have been reported exhibiting a good performance over an extended wavelength range (~100 nm) [18-20]. Nevertheless, these architectures imply trade-offs either in the performance or size of the mode converter and mux/demux.

Subwavelength grating (SWG) structures are an essential

Manuscript received XXXXXXX YY, 2021; revised XXXXXXX YY, 2021; accepted XXXXXXX YY, 2021. This work was supported in part by the Spanish Ministry of Science and Innovation (MICINN) under grants RTI2018-097957-B-C33, RED2018-102768-T, TEC2015-71127-C2-1-R (FPI BES-2016-077798) and NEOTEC-CDTI-SNEO20181232 (Alcyon Photonics S.L.); and the Community of Madrid – FEDER funds (S2018/NMT-4326). This project has received funding from the Horizon 2020 research and innovation program under Marie Sklodowska-Curie grant No. 734331. (*Corresponding author: David González-Andrade.*)

D. González-Andrade was with the Instituto de Óptica Daza de Valdés, Consejo Superior de Investigaciones Científicas (CSIC), Madrid 28006, Spain. He is now with the Centre de Nanosciences et de Nanotechnologies, CNRS, Université Paris-Sud, Université Paris-Saclay, Palaiseau 91120, France (email: david.gonzalez-andrade@c2n.upsaclay.fr).

R. Fernández de Cabo and A. V. Velasco are with the Instituto de Óptica Daza de Valdés, Consejo Superior de Investigaciones Científicas (CSIC), Madrid 28006, Spain (e-mail: r.fernandez@csic.es; a.villafranca@csic.es).

J. Vilas, I. Olivares and A. Dias are with Alcyon Photonics S.L., Madrid 28004, Spain (e-mail: j.vilas@alcyonphotonics.com; irene@alcyonphotonics .com; antonio.dias@alcyonphotonics.com).

J. M. Luque-González, J. G. Wangüemert-Pérez, A. Ortega-Moñux, Í. Molina-Fernández and R. Halir are with the Departamento de Ingeniería de Comunicaciones, ETSI Telecomunicación, Universidad de Málaga, Málaga 29071, Spain (e-mail: jmlg@ic.uma.es; gonzalo@ic.uma.es; aom@ic.uma.es; imf@ic.uma.es; rhalir@uma.es).

P. Cheben is with the National Research Council Canada, 1200 Montreal Road, Bldg. M50, Ottawa K1A 0R6, Canada (e-mail: Pavel.Cheben@nrc-cnrc.gc.ca).

Digital Object Identifier XX.XXXX/LPT.XXXX.XXXXXXX

tool for the realization of high-performance integrated photonic devices [21, 22]. SWG waveguides are an arrangement of different dielectric materials that alternate with a periodicity smaller than the operating wavelength. In this operation regime, diffractive effects are suppressed, enabling to engineer the optical properties of the equivalent metamaterial, i.e., refractive index, dispersion, and anisotropy [22]. In the mode-division multiplexing architectures, SWGs have been successfully applied to adiabatic couplers [23] and ADCs [24,25].

Taking advantage of the extended design space provided by SWG waveguides, we recently demonstrated a mode converter and mux/demux based on an SWG MMI, two trapezoidal tapers as 90° phase shifter and a symmetric Y-junction [26,27]. This architecture offers an optimized balance between insertion loss and operating bandwidth However, the crosstalk was limited in this architecture by the narrow spectral response of the conventional phase shifter.

In this Letter, we report on the design and realization of an MMI-based mode converter and mux/demux with a subwavelength-engineered phase shifter for extended broadband operation. The proposed device leverages the unique properties of SWG metamaterial waveguides to reduce not only the losses related to conventional MMIs but also the phase deviation induced by the conventional phase shifters when detuning from the design wavelength. The measured results show losses as low as 2 dB and crosstalk below -17 dB for a complete MDM link over a bandwidth of 245 nm.

II. Design And Simulations

Figure 1 shows a three-dimensional (3D) schematic of the proposed mode converter and mux/demux, which is based on an SWG MMI, an SWG phase shifter and a symmetric Y-junction. Considering operation as mux, the fundamental transverse-electric (TE_0) mode is injected through port 1 or port 2. When using port 1 as input, TE_0 mode is split by the SWG MMI with a 50:50 splitting ratio and a +90° phase difference between the upper and lower output arms. The SWG phase shifter introduces an additional –90° phase shift between the modes propagating through the upper and lower arms, resulting in two in-phase TE_0 modes. Theoretically, a symmetric Y-junction with a perfect sharp junction tip between the arms is a lossless and broadband power splitter/combiner. Thus, the two in-phase TE_0 modes are combined into the TE_0 mode of the stem waveguide (i.e., port 3). Similarly, the TE_0 mode at port 2 is split with a 50:50 ratio and a –90° phase difference between the upper and lower output arms of the MMI. Hence, after the phase shifter, a 180° phase difference is induced. The two out-of-phase TE_0 modes at the Y-junction arms are now combined into the TE_1 mode at port 3. A similar reasoning can be applied for demux operation. Since the symmetric Y-junction can perform the mode conversion in a wavelength-agnostic fashion in theory, loss and crosstalk of the entire device is ultimately limited by the performance of the MMI and the phase shifter. Here we use our broadband subwavelength-engineered MMI [27] while mitigating the limitation of wavelength-dependent spectral response of the phase shifter by controlling both anisotropy and dispersion using SWG metamaterial.

The mode converter and mux/demux is designed using 3D finite-difference time-domain (FDTD) simulations, following the approach detailed in [26,28], considering complete cladding filling. An in-depth study of the effect of air gaps in SiO_2 cladding can be found in [29]. For the MMI design, the beat length is controlled by judiciously selecting the duty cycle and pitch (Λ_{MMI}) of the SWG structure. A flat beat length spectral response is achieved for a duty cycle of 50% and $\Lambda_{MMI} = 0.19$ µm. SWG tapers have a length of $L_A = 5.7$ µm for efficient coupling between the interconnection waveguides of width $W_I = 0.5$ µm and the access waveguides of width $W_A = 1.7$ µm. The gap at the MMI output is $G_S = 0.3$ µm to avoid power coupling. Low loss and imbalance over a 300 nm wavelength range is achieved by optimizing both length ($L_{MMI} = 15.2$ µm) and width ($W_{MMI} = 3.25$ µm) of the MMI. The symmetric Y-junction is connected to the phase shifter through two adiabatic tapers ($L_T = 2$ µm), while reducing the width from $W_I = 0.5$ µm to $W_Y = 0.4$ µm to avoid the excitation of higher-order modes in the multimode waveguide. Negligible losses are achieved for an arm length of $L_Y = 7.14$ µm and a final separation between the arms of $G_Y = 1.6$ µm. Further details of design can be found in Ref. [27].

The broadband phase shifter comprises two parallel SWG waveguides of dissimilar widths ($W_U = 1.8$ µm and $W_L = 1.6$ µm) but with the same length (L_{PS}), period (Λ_{PS}) and duty cycle [30]. The wavelength variation of the phase shift induced by the parallel SWG waveguides can be engineered by selecting the SWG period and duty cycle. We chose a duty cycle of 50% to maximize the minimum feature size of the SWG segments and found that $\Lambda_{PS} = 0.2$ µm yields a minimum phase shift deviation from the target –90°. Furthermore, an adiabatic transition between interconnection strip waveguides and the SWG waveguides is required. For this purpose, we use SWG tapers with a length of $L_B = 3$ µm and optimize the length of the parallel SWG waveguides ($L_{PS} = 16.8$ µm) to compensate for the phase shift introduced by the SWG tapers.

Figure 2 shows a performance comparison between our

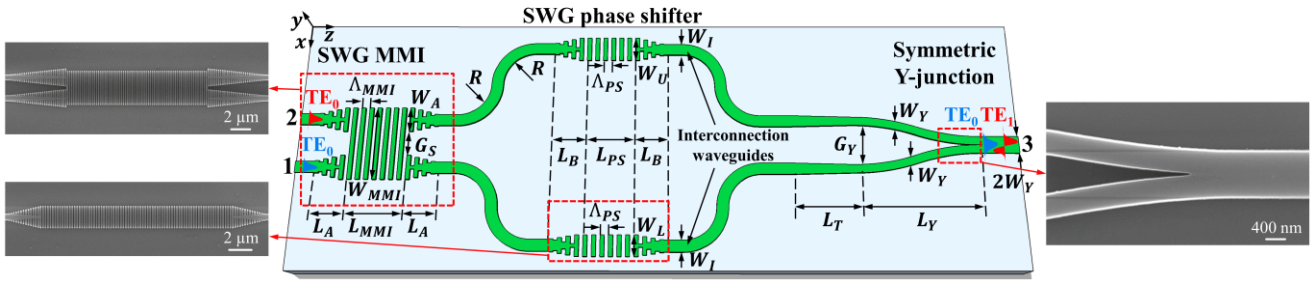

Fig. 1. Schematic of the mode converter and mux/demux. Insets: SEM images of the SWG MMI, SWG phase shifter and symmetric Y-junction.

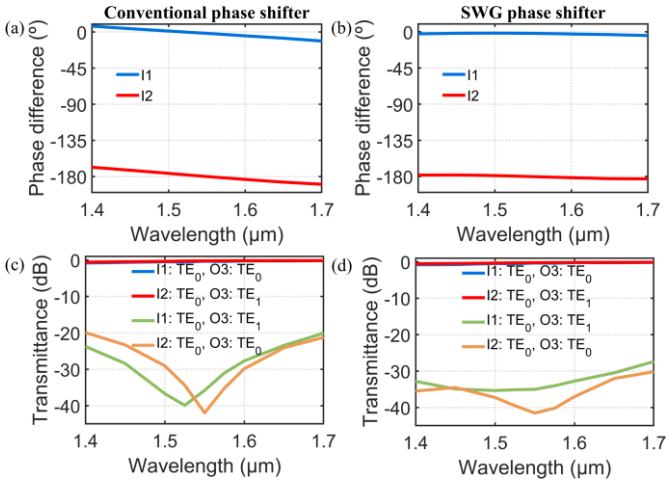

Fig. 2. Calculated phase difference between the two TE_0 modes at the Y-junction arms when using (a) a conventional phase shifter and (b) an SWG phase shifter. Simulated transmittance of the mode converter and mux/demux with (c) a conventional phase shifter and (d) an SWG phase shifter.

device with SWG phase shifter and a device based on a conventional phase shifter [27]. In our device, the low phase errors of both the SWG MMI and SWG phase shifter yield negligible deviations with respect to target 0 and 180° phase difference within the entire simulated bandwidth (see Figs. 2(a) and 2(b)). Our device exhibits a substantially reduced crosstalk within the 300 nm bandwidth (1.4 – 1.7 μm) with values below -30.2 dB and -27.4 dB for TE_0 and TE_1 mode conversion, respectively (see Figs. 2(c) and 2(d)). The performance is hardly degraded for duty cycle variations of < 10%, as the SWG MMI exhibits losses and imbalance below 1 dB, and a phase error below 5° [28], and the flat spectral response of the SWG phase shifter is maintained within the 1.4 – 1.7 μm range [30].

III. Fabrication And Experimental Characterization

The device was fabricated in a commercial foundry using SOI wafers with a silicon thickness of 220 nm and a 2 μm buried oxide (BOX). The patterning process was carried out with a 100 keV electron-beam lithography system and transferred to the silicon layer using an anisotropic reactive ion etching process. Scanning electron microscope (SEM) images of different parts of the device were taken before cladding deposition (see insets of Fig. 1). A 2.2 μm thick SiO_2 cladding oxide was deposited afterwards by chemical vapour deposition. Smooth facets were created with a deep-etch process, enabling efficient light coupling in and out of the chip via high-performance SWG edge couplers [31].

The setup used for experimental characterization is shown in Fig. 3(a). A complete MDM link was used as test structure, including two mode converters and mux/demux in back-to-back configuration connected via a 600-μm-long multimode waveguide. Two tunable lasers were employed for the 1.41 – 1.68 μm wavelength range. The polarization of the light was controlled with a three-paddle fiber polarization controller, a linear polarizer and a half-wave plate. A lensed polarization maintaining fiber was used to couple the light to the chip. We verified that TE polarization was injected at the chip input by means of a free-space polarimeter. At the chip output the light was collimated with a 40x microscope objective, and the polarization was monitored with a Glan-Thompson polarizer. The output beam was then directed either to a germanium photodetector or an infrared camera, with a mirror on a folding mount. We measured the transmittance of the complete MDM system and a reference waveguide with the same length and number of bends as the MDM link. Figure 3(b) shows the transmittance spectra of the nominal flavour after the normalization process for input ports 1 and 2. For comparison we have shown in Fig. 3(c) the measurements of the MDM with conventional phase shifter [27]. Insertion loss and crosstalk of the complete MDM link are under 2 dB (i.e., <1 dB per device) and -17.2 dB in the 1427 – 1672 nm wavelength range, respectively, for TE_0 mode mux-demux (input port 1). These values decrease up to 1.2 dB (i.e., 0.6 dB per device) and -18.1 dB for TE_1 mode mux-demux (input port 2). A comparison of state-of-the-art two-mode MDM links is provided in Table I. Although most devices operate in a bandwidth of less than 100 nm, architectures based on counter-tapered couplers [7], SWG adiabatic couplers [23] and SWG MMIs [27] have reported operation over a wavelength range broader than 120 nm. Our device is, to the best of our knowledge, among the mode converters and mux/demux with broadest bandwidth.

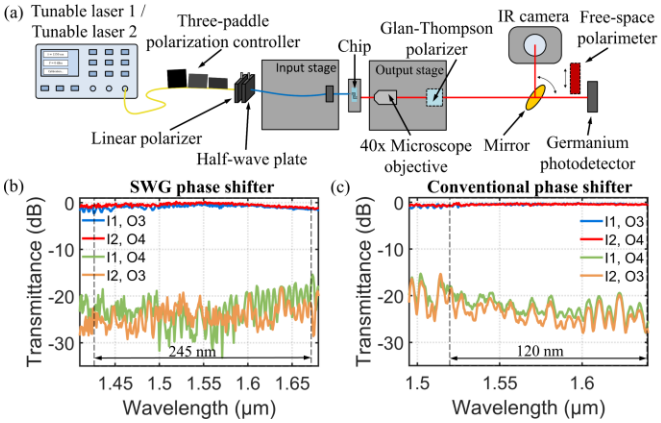

Fig. 3. (a) Schematic of the setup used to characterize the MDM link. Measured transmittance of the MDM link with (b) an SWG phase shifter and (c) a conventional phase shifter [27].

TABLE I
Comparison of State-of-the-Art Two-Mode MDM Links

Ref	Insertion loss [dB]	Crosstalk [dB]	Bandwidth [nm]	Mux length [μm]
[6]	> 0.3	< -16	100	50
[7]	< 1.0	< -13	180	260
[8]	< 1.1	< -24	100	150
[10]	< 1.5	<-9	100	> 100
[11]	> 0.4	< 9.1	106	60
[12]	< 2.4	< -12	100	4.22
[13]	< 1.0	< -24	60	3
[14]	< 2.0	< -12.5	100	2.55
[15]	~ 0.3	< -36	100	300
[16]	~ 1.0	< -20	75	200
[17]	< 1.5	< -19	90	181
[23]	< 2.6	< -18.8	230	55
[27]	< 1.1	< -18	120	38.6
This work	< 2.0	< -17.2	245	78.6

IV. Conclusion

In summary, we have reported a broadband mode converter and mux/demux based on subwavelength-engineered phase shifter and MMI, and a symmetric Y-junction. While the wavelength-dependent beat length of conventional MMIs mainly accounts for the losses of this MDM architecture, the phase shifter performance is a key factor for achieving low crosstalk. The additional degree of freedom provided by subwavelength engineering allows to control the metamaterial dispersion and anisotropy, enhancing the performance of the MMI and phase shifter by judiciously selecting their geometrical parameters. We fabricated and characterized a full MDM link, which exhibited insertion loss under 2 dB and crosstalk better than -17 dB in a measured bandwidth of 245 nm for both TE_0 and TE_1 modes. Compared with the state-of-the-art mode converters and mux/demux, our device achieves an outstanding operating bandwidth of 245 nm, which is 125 nm larger compared to a device with a conventional phase shifter [27]. We believe that these results will pave the way for ultra-dense optical transmission and high-speed data computing in the next generation of data centers.

References

[1] G. Wetzstein, A. Ozcan, S. Gigan, S. Fan, D. Englund, M. Slojačić, C. Denz, D. A. B. Miller, and D. Psaltis, "Inference in artificial intelligence with deep optics and photonics," *Nature*, vol. 588, no. 7836, pp. 39–47, Dec. 2020.

[2] A. A. Aboketaf, A. W. Elshaari, and S. F. Preble, "Optical time division multiplexer on silicon chip," *Opt. Express*, vol. 18, no. 13, pp. 13529–13535, Jun. 2010.

[3] S. Chen, Y. Shi, S. He, and D. Dai, "Compact monolithically-integrated hybrid (de)multiplexer based on silicon-on-insulator nanowires for PDM-WDM systems," *Opt. Express*, vol. 23, no. 10, pp. 12840–12849, May 2015.

[4] C. Li, D. Liu, and D. Dai, "Multimode silicon photonics," *Nanophotonics*, vol. 8, no. 2, pp. 227–247, Nov. 2019.

[5] D. Dai, J. Wang, and Y. Shi, "Silicon mode (de)multiplexer enabling high capacity photonic networks-on-chip with a single-wavelength-carrier light," *Opt. Lett.*, vol. 38, no. 9, pp. 1422–1424, May 2013.

[6] Y. Ding, J. Xu, F. Da Ros, B. Huang, H. Ou, and C. Peucheret, "On-chip two-mode division multiplexing using tapered directional coupler-based mode multiplexer and demultiplexer," *Opt. Express*, vol. 21, no. 8, pp. 10376–10382, Apr. 2013.

[7] J. Wang, Y. Xuan, M. Qi, H. Huang, Y. Li, M. Li, X. Chen, Z. Sheng, A. Wu, W. Li, X. Wang, S. Zou, and F. Gan, "Broadband and fabrication-tolerant on-chip scalable mode-division multiplexing based on mode-evolution counter-tapered couplers," *Opt. Lett.*, vol. 40, no. 9, pp. 1956–1959, May 2015.

[8] D. Guo and T. Chu, "Silicon mode (de)multiplexers with parameters optimized using shortcuts to adiabaticity," *Opt. Express*, vol. 25, no. 8, pp. 9160–9170, Apr. 2017.

[9] D. Dai, C. Li, S. Wang, H. Wu, Y. Shi, Z. Wu, S. Gao, T. Dai, H. Yu, and H.-K. Tsang, "10-Channel mode (de)multiplexer with dual polarizations," *Laser Photon. Rev.*, vol. 12, no. 1, p. 1700109, Nov. 2017.

[10] J. B. Driscoll, R. R. Grote, B. Souhan, J. I. Dadap, M. Lu, and R. M. Osgood, Jr., "Asymmetric Y-junctions in silicon waveguides for on-chip mode-division multiplexing," *Opt. Lett.*, vol. 38, no. 11, pp. 1854–1856, Jun. 2013.

[11] H. Li, P. Wang, T. Yang, T. Dai, G. Wang, S. Li, W. Chen, and J. Yang, "Experimental demonstration of a broadband two-mode multi/demultiplexer based on asymmetric Y-junctions," *Opt. Laser Technol.*, vol. 100, pp. 7–11, Mar. 2018.

[12] L. F. Frellsen, Y. Ding, O. Sigmund, and L. H. Frandsen, "Topology optimized mode multiplexing in silicon-om-insulator photonic wire waveguides," *Opt. Express*, vol. 24, no. 15, pp. 16866–16873, Jul. 2016.

[13] W. Chang, L. Lu, X. Ren, D. Li, Z. Pan, M. Cheng, D. Liu, and M. Zhang, "Ultra-compact mode (de) multiplexer based on subwavelength asymmetric Y-junction," *Opt. Express*, vol. 26, no. 7, pp. 8162–8170, Apr. 2018.

[14] A. Y. Piggott, E. Y. Ma, L. Su, G. H. Ahn, N. V. Sapra, D. Vercruysse, A. M. Netherton, A. S. P. Khope, J. E. Bowers, and J. Vučković, "Inverse-designed photonics for semiconductor foundries," *ACS Photonics*, vol. 7, no. 3, pp. 569–575, Feb. 2020.

[15] J. Xing, Z. Li, X. Xiao, J. Yu, and Y. Yu, "Two-mode multiplexer and demultiplexer based on adiabatic couplers," *Opt. Lett.*, vol. 38, no. 17, pp. 3468–3470, Sep. 2013.

[16] C. Sun, Y. Yu, M. Ye, G. Chen, and X. Zhang, "An ultra-low crosstalk and broadband two-mode (de) multiplexer based on adiabatic couplers," *Sci. Rep.*, vol. 6, p. 38494, Dec. 2016.

[17] Z. Zhang, Y. Yu, and S. Fu, "Broadband on-chip mode-division multiplexer based on adiabatic couplers and symmetric Y-junction," *IEEE Photonics J.*, vol. 9, no. 2, p. 6600406, Feb. 2017.

[18] T. Uematsu, Y. Ishizaka, Y. Kawaguchi, K. Saitoh, and M. Koshiba, "Design of a compact two-mode multi/demultiplexer consisting of multimode interference waveguides and a wavelength-insensitive phase shifter for mode-division multiplexing transmission," *J. Lightw. Technol.*, vol. 30, pp. 2421–2426, May 2012.

[19] Y. Li, C. Li, C. Li, B. Cheng, and C. Xue, "Compact two-mode (de)multiplexer based on symmetric Y-junction and multimode interference waveguides," *Opt. Express*, vol. 22, no. 5, pp. 5781–5786, Mar. 2014.

[20] L. Han, S. Liang, H. Zhu, L. Qiao, J. Xu, and W. Wang, "Two-mode de/multiplexer based on multimode interference couplers with a tilted joint as phase shifter," *Opt. Lett.*, vol. 40, no. 4, pp. 518–521, Feb. 2015.

[21] R. Halir, A. Ortega-Moñux, D. Benedikovic, G. Z. Mashanovich, J. G. Wangüemert-Pérez, J. H. Schmid, I. Molina-Fernández, and P. Cheben, "Subwavelength-grating metamaterial structures for silicon photonic devices," *Proc. IEEE*, vol. 106, no. 12, pp. 2144–2157, Aug. 2018.

[22] P. Cheben, R. Halir, J. H. Schmid, H. A. Atwater, and D. R. Smith, "Subwavelength integrated photonics," *Nature*, vol. 560, no. 7720, pp. 565–572, Aug. 2018.

[23] L. Xu, Y. Wang, D. Mao, J. Zhang, Z. Xing, E. El-Fiky, M. G. Saber, A. Kumar, Y. D'Mello, M. Jacques, and D. V. Plant, "Ultra-broadband and compact two-mode multiplexer based on subwavelength-grating-slot-assisted adiabatic coupler for the silicon-on-insulator platform," *J. Lightw. Technol.*, vol. 37, no. 23, pp. 5790–5800, Sep. 2019.

[24] Z. Jafari, A. Zarifkar, and M. Miri, "Compact fabrication-tolerant subwavelength-grating-based two-mode division (de)multiplexer," *Appl. Opt.*, vol. 56, no. 26, pp. 7311–7319, Sep. 2017.

[25] W. Jiang, J. Miao, T. Li, and L. Ma, "On-chip silicon dual-mode multiplexer via a subwavelength grating-based directional coupler and a mode blocker," *Appl. Opt.*, vol. 58, no. 33, pp. 9290–9296, Nov. 2019.

[26] D. González-Andrade, J. G. Wangüemert-Pérez, A. V. Velasco, A. Ortega-Moñux, A. Herrero-Bermello, I. Molina-Fernández, R. Halir, and P. Cheben, "Ultra-broadband mode converter and multiplexer based on sub-wavelength structures," *IEEE Photonics J.*, vol. 10, no. 2, p. 2201010, Apr. 2018.

[27] D. González-Andrade, A. Dias, J. G. Wangüemert-Pérez, A. Ortega-Moñux, I. Molina-Fernández, R. Halir, P. Cheben, and A. V. Velasco, "Experimental demonstration of a broadband mode converter and multiplexer based on subwavelength grating waveguides," *Opt. Laser Technol.*, vol. 129, p. 106297, Apr. 2020.

[28] R. Halir, P. Cheben, J. M. Luque-González, J. D. Sarmiento-Merenguel, J. H. Schmid, G. Wangüemert-Pérez, D.-X. Xu, S. Wang, A. Ortega-Moñux, and I. Molina-Fernández, "Ultra-broadband nanophotonic beamsplitter using an anisotropic sub-wavelength metamaterial," *Laser Photon. Rev.*, vol.10, no. 6, pp. 1039–1046, Nov. 2016.

[29] H. Shiran, H. R. Mojaver, J. Bachman, C. Jin, and O. Liboiron-Ladouceur, "Impact of SiO2 cladding voids in SiPh building blocks," in *2020 IEEE Photonics Conference* (IPC), Vancouver, BC, Canada, 2020, pp. 215-216.

[30] D. González-Andrade, J. M. Luque-González, J. G. Wangüemert-Pérez, A. Ortega-Moñux, P. Cheben, I Molina-Fernández, and A. V. Velasco, "Ultra-broadband nanophotonic phase shifter based on subwavelength metamaterial waveguides," *Photon. Res.*, vol. 3, no. 3, pp. 359–367, Mar. 2020.

[31] P. Cheben J. H. Schmid, S. Wang, D.-X. Xu, M. Vachon, S. Janz, J. Lapointe, Y. Painchaud, and M. J. Picard, "Broadband polarization independent nanophotonic coupler for silicon waveguides with ultra-high efficiency," *Opt. Express*, vol. 23, no. 17, pp. 22553–22563, Aug. 2015.